ISSN 1996-3416

International Journal of Chemical Technology

http://knowledgiascientific.com

Knowledgia SCIENTIFIC
A Place to Publish Outstanding Research

International Journal of Chemical Technology 4 (1): 17-30, 2012
ISSN 1996-3416 / DOI: 10.3923/ijct.2012.17.30

Prevention of Steel Corrosion by Cathodic Protection Techniques

[1]Anees A. Khadom and [2]Khalid W. Hameed
[1]Department of Mechanical Engineering, College of Engineering, University of Daiyla, Baquba 32001, Daiyla, Iraq
[2]Department of Chemical Engineering, College of Engineering, University of Baghdad, Aljadrea 71001, Baghdad, Iraq

Corresponding Author: Anees A. Khadom, Department of Mechanical Engineering, College of Engineering, University of Daiyla, Baquba 32001, Daiyla, Iraq Tel: 00964 790 2305786

ABSTRACT

The purpose of this study, was to investigate the application of sacrificial anode and impressed current cathodic protection techniques as a tool for determining the optimum zinc consumption, protection potential and protection current for steel in saline water at a given environment of temperature, time, pH and solution velocity. Weight loss method was used to determine the amount of zinc consumption, while the electrochemical polarization methods were used to determine the protection current and potential. Box-Wilson experimental design was used to design the set of impressed current experiments. Zinc consumption increase with temperature, time and solution velocity, while it decreases with pH of solution. Protection potential and current were analyzed using mathematical models. These models were estimated by regression analysis methods.

Key words: Steel, zinc, weight loss, polarization, cathodic protection

INTRODUCTION

Among the various corrosion control methods available, cathodic protection is a major technique adopted to control the corrosion of steel. Cathodic protection system is aimed to shift the potential of the steel to the least probable range for corrosion (Parthiban *et al*., 2008). In practice, it is most commonly used to protect ferrous materials and predominantly carbon steel (Lindley and Rudd, 2001). One of the most corrosive environments is the saline water (Zahran and Sedahmed, 1997). Equipment used in these environments, such as desalination industry and cooling systems using seawater as a coolant suffer severely from corrosion owing to the presence of the highly aggressive chloride ions in high concentration. Chloride ions have the ability of destroying oxide films which may protect metals such as steel, stainless steel and copper and its alloys. To overcome this problem two approaches are possible, namely: (1) either use expensive alloys to build desalination equipments; or (2) to use cheaper alloys along with cathodic protection. The use of expensive alloys in building equipment increases the capital costs of the plant. In most of the cases it was found that using low cost alloys along with cathodic protection is more cost effective than using expensive alloys. There most important types of cathodic protection are the Impressed Current Cathodic Protection (ICCP) and Sacrificial Anode Cathodic Protection (SACP), also known as galvanic cathodic protection. In ICCP, direct current (dc) source is connected with its positive terminal to the auxiliary electrode (anode) and its negative terminal to the structure to be protected; in this way, current flows from the electrode through the electrolyte to the structure. While in SACP, the

auxiliary anode is composed of a metal more active in the Galvanic Series than the metal to be protected and the impressed source of current can then be omitted. Sacrificial metals used for cathodic protection consist of magnesium-base and aluminum-base alloys and, zinc. Sacrificial anodes serve essentially as sources of portable electrical energy. They are useful particularly when electric power is not readily available, or in situations where it is not convenient or economical to install power lines for the purpose (Shrier, 2000). The saline and acidic are very corrosive environment and the study of corrosion inhibition process is very important (Omotosho *et al*., 2012; Ekuma *et al*., 2007, 2008; Alagbe *et al*., 2006; Bazargan-Lari and Bazargan-Lari, 2009). The present study, was an attempt to apply the above two cathodic protection methods for the corrosion prevention of steel pipe carrying saline water. The effect of temperature, flow rate, pH and time were studied in present work.

MATERIALS AND METHODS

Sacrificial anode system: Experimental work of sacrificial anode system was carried out to determine the consumption rate of zinc in artificial sea water (4% w/v NaCl/distilled water) using weight loss for various conditions of temperature (0-45°C), flow rate (5-900 L h^{-1}), pH (2-12) and time (1-4 h). Working electrode was tube specimen of low carbon steel with dimensions of 13.50 cm length, 2.68 cm inside diameter and 0.31 cm thick. The composition of steel specimen was as follows: wt.%, C, 0.1648; Si, 0.2540; Mn, 0.5101; S, 0.0062; Cr, 0.0253; Ni, 0.0090; Cu, 0.1511, V, 0.0034 and the remainder is Fe. Anode electrode was zinc strip with dimensions of 12.50 cm length, 1.00 cm width and 0.60 cm thick. The composition of zinc specimen was as follows: wt.%, Al, 0.12; Pb, 0.0034; Cu, 0.0017; Cd, 0.0033; Fe, 0.0032; Sn, 0.0023 and the remainder is Zn. The cleaning procedure of low carbon steel tubes (cathode) and zinc strips (anode) before and after each experimental test was done as mentioned everywhere (Yaro *et al*., 2011a; Khadom *et al*., 2010). The apparatus shown in Fig. 1 was used to obtain the experimental data. After adjusting the operating conditions, the zinc strip was weighted and fixed at the inlet of the steel tube by rubber stopper and was electrically connected by an insulated copper wire to the steel tube outlet. The zinc strip is extending along the steel tube to ensure uniform current and potential distribution along the tube wall. The seawater was pumped from the vessel through the flow meter to measure the

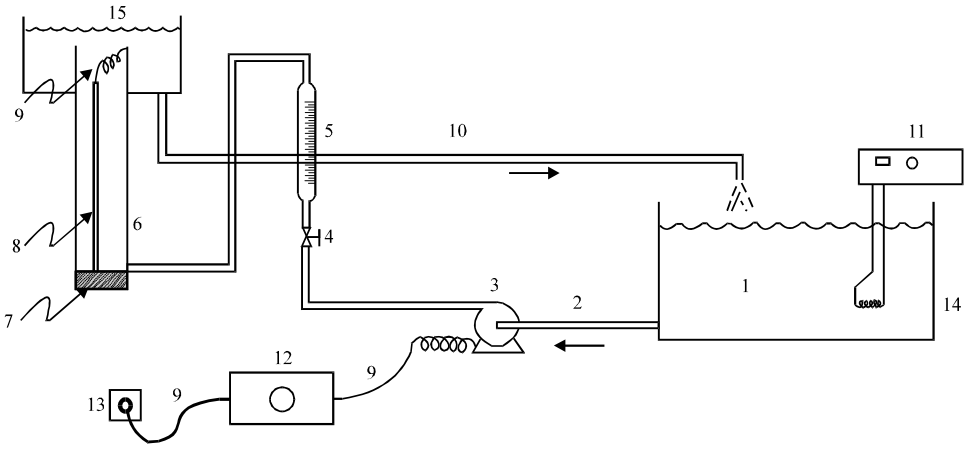

1. Electrolyte (seawater)	2. feed forward pipe	3. Pump	4. value	5. Rota meter
6. Tube steel	7. Rubber stopper	8. Zinc strip	9. Copper wire	10. Feedback pipe
11. Heater or chiller	12. Variac	13. Electric source	14. Insulated vessel	15. Overflow

Fig. 1: Schematic diagram of apparatus used in sacrificial anode test system

desired flow rate, then it flow from the bottom to the top of steel tube to return to the vessel again. After each run the zinc strip was rinsed in distilled water and brush to remove the corrosion products, dried with clean tissue then immersed in the benzene and acetone, dried again and then re-weighted to determine the weight loss. The steel tube is cleaned in similar way.

Impressed current system: For impressed current system, the experimental work was carried out to determine the potential and current density required in cathodic protection using weight loss and polarization techniques for various conditions of temperature (0-45°C), rotating velocity (0-400 rpm) and pH (2-12). Working electrode was cylinder specimen of low carbon steel with dimensions of 1.58 cm length, 2.33 cm outside diameter and 0.18 cm thick having the same above chemical composition. Auxiliary electrode was a rod of high conductivity graphite, 4.50 cm length and 0.8 cm outside diameter. The cathodic potential is determined with respect to Saturated Calomel Electrode (SCE). A lugging capillary bridge leading to the reference electrode is mounted near the center of cathode to within 1 mm from the side of the cathode. The opening of the capillary tube near the cathode is equal to 1 mm in diameter. The rotating shaft was made of brass and Teflon. The steel specimen was mounted between two Teflon spaces fitted with O-ring seals to prevent electrolyte contacting the brass rod. The electrical contact to the cylindrical specimen was made through the rotor and a carbon brush contact. Electrochemical cell: Consists of a spherical flask with six necks, one with large opening located in the middle used to input the shaft which combined with steel specimen and the others with smaller openings located around the middle large opening. One of them was used to input the reference electrode, one was used for thermometer, two were used for auxiliary electrodes and the latter was used for aerated. The capacity of electrochemical cell is 1 L. Apparatus shown in Fig. 2 was used to find polarization curves, protection potential and protection current.

RESULTS AND DISCUSSION

Sacrificial anode system: To investigate the rate of zinc consumption during the cathodic protection of carbon steel pipe carrying 4% NaCl solution, 256 experiments were conducted using the factorial experimental design, each variable was discrete into four levels, such that for temperature (0, 15, 30, 45 °C), flow rate (5, 300, 600, 900 L h^{-1}), pH (2, 5, 8, 12) and time (1, 2, 3, 4 h). For the present system the electrochemical cell responsible for cathodic protection is Zn/NaCl/Fe. The anodic reaction is:

$$Zn \rightarrow Zn^{+2} + 2e \quad (1)$$

and the cathodic reaction is one of the following reactions:

$$2H^{+} + 2e \rightarrow H_2 \uparrow \quad (2)$$

$$2H_2O + 2e \rightarrow H_2 \uparrow + 2OH^{-} \quad (3)$$

$$O_2 + 2H_2O + 4e \rightarrow 4OH^{-} \quad (4)$$

The cathodic reaction is depending on the nature of seawater but reaction of O_2 reduction towards the wall of the carbon steel pipe is assumed predominate.

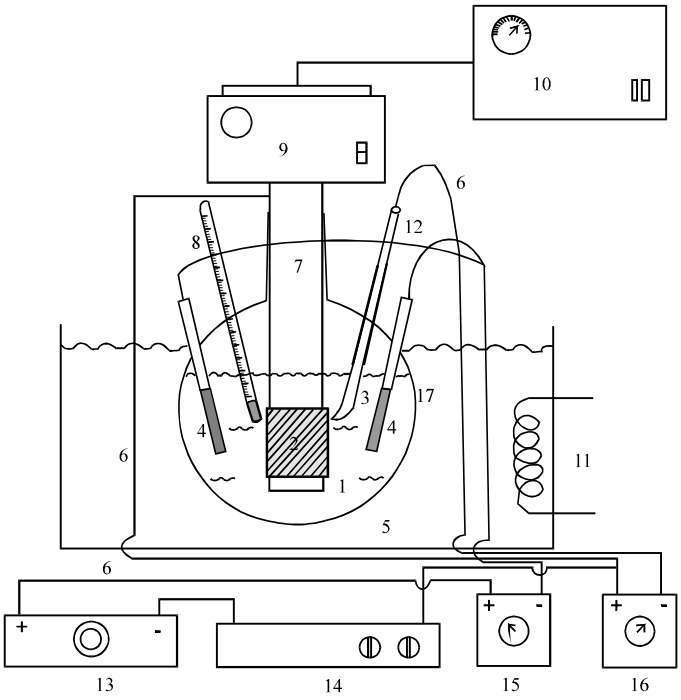

1. Electrollyte (sea water)	2. Cylinder steel specimen	3. Luggin	4. Auxiliary anode (Graphite)	5. water bath
6. wires	7. Shalf motor	8. Thermometer	9. Motor	10. Speed control
11. heating or cooling coil	12. SCE	Power supply	14. Box resistance	15. A meter
16. Voltmeter				

Fig. 2: Schematic diagram of apparatus used in impressed current test system

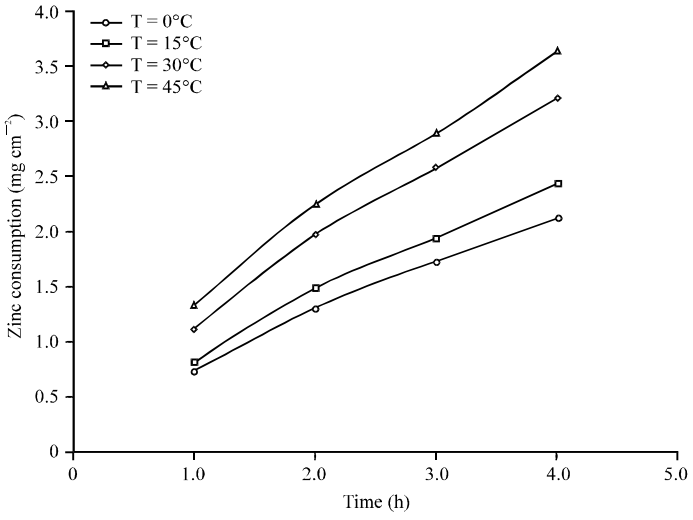

Fig. 3: Zinc consumption with time for different temperatures at flow rate = 600 L h^{-1} and pH = 8

Time effect: Figure 3 shows the rate of zinc consumption (dissolution) which is instead of corrosion rate of steel, with time at different temperatures, different flow rates and different pH, respectively.

The rate of zinc dissolution increases with increasing time and this is a normal case. But this increasing is not equally with time where the dissolution rate in the first hour is more than second hour and so on. The reasons of that are attributed to continuous growth of the corrosion products layer with time which affects the transport of oxygen to the metal surface and the activity of the surface and hence the corrosion rate. Also, the cathodic reactions will result an increase in pH with time either by the removal of hydrogen ions Eq. 2 or by the generation of hydroxyl ions Eq. 2 and 4, both reasons are reduced the corrosion rate of steel and hence the dissolution rate of zinc.

Temperature effect: Figure 4 shows the effect of temperature on the rate of zinc dissolution with time with different flow rates and with different pH's, respectively. The increase in the rate of zinc dissolution with increasing seawater temperature (particularly from 15 to 30°C) may be explained in terms of the following effects:

- A temperature increase usually increases the reaction rate which is the corrosion rate and according to the Freundlich equation (Shrier, 2000):

$$\text{Corrosion rate} = k\, C_{O_2}^{n} \tag{5}$$

The rate constant (k) varying with temperature according to Arrhenius equation:

$$k = k_0 e^{-E/RT} \tag{6}$$

Equation 5 and 6 indicate that the k is increased with increasing temperature and then the corrosion rate which leads to increasing the rate of zinc dissolutions.

- Increasing seawater temperature leads to decreasing seawater viscosity with a consequent increase in oxygen diffusivity according to stokes-Einstein equation (Konsowa and El-Shazly, 2002):

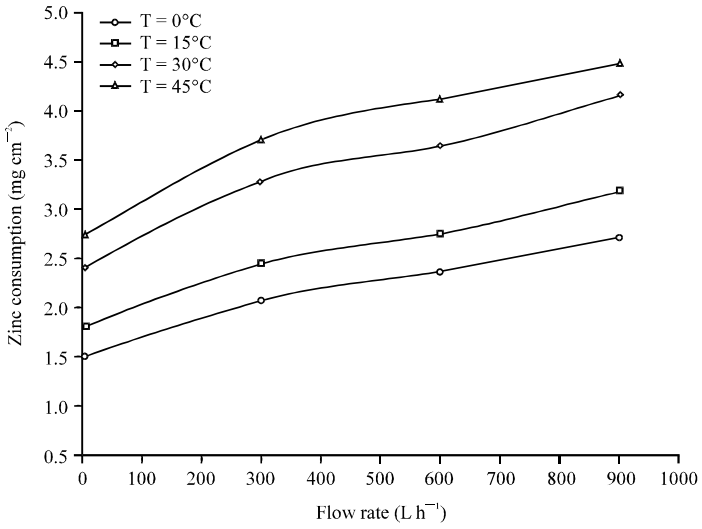

Fig. 4: Zinc consumption with flow rate for different temperatures at time = 4 h and pH = 5

$$k = k_o e^{-E/RT} \frac{\mu D}{T} = \text{constant} \quad (7)$$

As a result of increasing the diffusivity of dissolved oxygen, the rate of mass transfer of dissolved oxygen to the cathode surface increases according to the following equation:

$$J = k_d C_{O_2} = \frac{D}{\delta_d} C_{O_2} \quad (8)$$

With a consequence increase in the rate of zinc dissolution.

- The decreases in seawater viscosity with increasing temperature improve the seawater conductivity with a consequent increase in corrosion current and the rate of corrosion
- On the other hand, increase of temperature reduces the solubility of dissolved oxygen with a subsequent decrease in the rate of oxygen diffusion to the cathode surface and the rate of corrosion

It seems that within the present range of temperature effects 1, 2 and 3 are predominating.

Flow rate effect: Figure 5 shows the effect of solution flow rate on the zinc dissolution with time, with different temperatures and with different pH's, respectively. It can be seen that the dissolution rate of zinc increases with increasing the flow rate. This may be attributed to the decrease in the thickness of hydrodynamic boundary layer and diffusion layer across which dissolved oxygen diffuses to the tube wall of steel with consequent increase in the rate of oxygen diffusion which is given by Eq. 8. Then the surface film resistance almost vanishes, oxygen depolarization, the products of corrosion and protective film are continuously swept away and continuous corrosion occurs. The flow rate of seawater may also caused erosion which combined with electrochemical attack (Khadom, 2010).

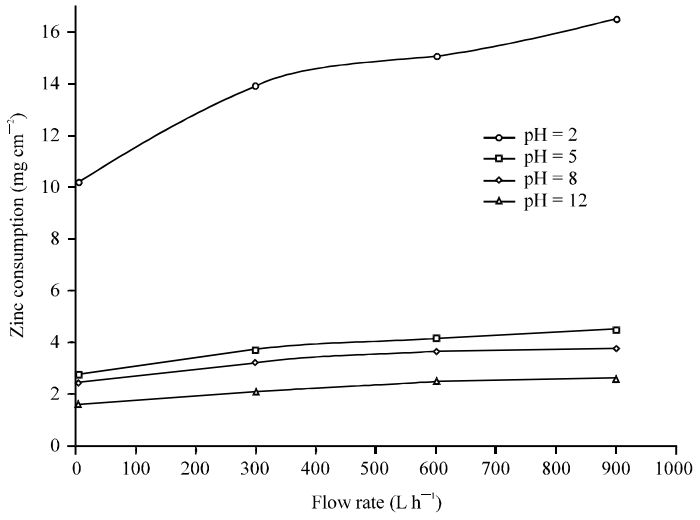

Fig. 5: Zinc consumption with flow rate for different pH's at time = 4 h and temperature = 45°C

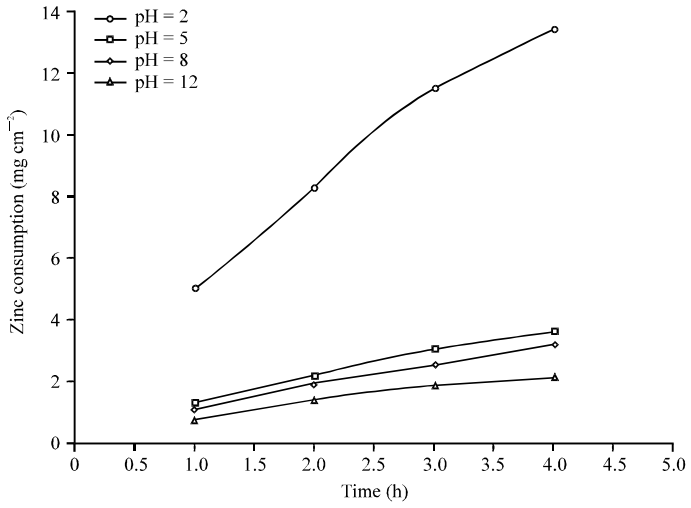

Fig. 6: Zinc consumption with time for different pH's at temperature 30°C and flow rate = 600 L h^{-1}

pH effect: Figure 6 shows the effect of pH on dissolution of zinc with time, with different temperatures and with different flow rates, respectively. It can be seen from this figure that the rate of zinc dissolution increases with decreasing of pH (particularly at range of pH 5 to 2). Within the range of about 5 to 12 the corrosion rate of steel and hence dissolution rate of zinc is slightly dependent of the pH, where it depends almost on how oxygen rapidly reaches to the metal surface. Although it was expected that at very high of pH value (12), the dissolution rate of zinc is much reducing because the steel becomes increasingly passive in present of alkalis and dissolved oxygen, but the nature of electrolyte (sea water) prevents that where chloride ions depassivate iron even at high pH. Within the acidic region (pH<5) the ferrous oxide film (resulting from corrosion) is dissolved, the surface pH falls and steel is more direct contact with environment. The increased rate of reaction (corrosion) is then the sum of both an appreciable rate of hydrogen evolution and oxygen depolarization. These results agree with our previous work (Yaro *et al.*, 2011a).

Impressed current system: Mathematical modeling was used every where to develop a relation among variables (Khadom *et al.*, 2009; Okeniyi *et al.*, 2012). To investigate the protection potential and protection current required for cathodic protection. Statistical and Central composite rotatable design (Box-Wilson) (Ahmed *et al.*, 2009; Ekuma and Idenyi, 2007; Ekuma, 2008) were adopted to design the set of experiments. For the purpose of design the operating range of variables are first specified according to the following:

- X_1: Temperature range between 0 to 45°C
- X_2: Rotating velocity range between 0 to 400 rpm
- X_3: pH range between 2 to 12

Number of experiments (N) is calculated according to the following equation depending on the number of variables, p, (X_1, X_2 and X_3):

$$N = 2^p + 2p + 1 \quad (9)$$

The relationship between the coded variables (X_j, where j = 1, 2, 3) and the corresponding real variables were:

$$X_{coded} = \frac{X_{actual} - X_{center}}{\left[\frac{X_{center} - X_{min}}{\sqrt{p}}\right]} \quad (10)$$

$$X_{1,coded} = \frac{X_{1,actual} - 22.5}{13} \quad (11)$$

$$X_{2,coded} = \frac{X_{2,actual} - 200}{115.5} \quad (12)$$

$$X_{3,coded} = \frac{X_{3,actual} - 7}{2.89} \quad (13)$$

Table 1 shows the coded and real values of the experiments to be conducted.

Protection potential E_p: To find the potential required in cathodic protection, the weight loss technique is adopted. The experimental results of the Corrosion Rate (CR) of steel cylinder specimen at different conditions without impressed current were shown in Table 2. The results show increase in corrosion rate of steel with increasing temperature and rotating velocity while there is a pronounced decrease with pH increase. The reasons of that are similar as mentioned above. Mathematical and statistical analysis are powerful way for representing the dependent and

Table 1: Coded and real values of experiments according to central composite rotatable design (3-variables)

	X_1		X_2		X_3	
Run No.	Coded	Real	Coded	Real	Coded	Real
1	-1	9.5	-1	85	-1	4.11
2	-1	9.5	-1	85	+1	9.89
3	-1	9.5	+1	315	-1	4.11
4	-1	9.5	+1	315	+1	9.89
5	+1	35.5	-1	85	-1	4.11
6	+1	35.5	-1	85	+1	9.89
7	+1	35.5	+1	315	-1	4.11
8	+1	35.5	+1	315	+1	9.89
9	-1.732	0	0	200	0	7
10	+1.732	45	0	200	0	7
11	0	22.5	-1.732	0	0	7
12	0	22.5	+1.732	400	0	7
13	0	22.5	0	200	-1.732	2
14	0	22.5	0	200	+1.732	12
15-18*	0	22.5	0	200	0	7

*Center point is repeated 3 times to asses experimental reproducibility

Table 2: Corrosion rate (CR) experimental results for designed variables expressed as corrosion rates (by weight loss) in absence of applying impressed current

Run No.	X_1	X_2	X_3	W_1 (g)	W_2 (g)	ΔW (mg)	CR (mdd)*
1	9.5	85	4.11	14.3721	14.3697	2.40	124.016
2	9.5	85	9.89	14.3732	14.3713	1.90	98.192
3	9.5	315	4.11	14.3725	14.3697	2.80	144.687
4	9.5	315	9.89	14.1320	14.1298	2.20	113.683
5	35.5	85	4.11	14.1318	14.1293	2.50	129.185
6	35.5	85	9.89	14.1322	14.1301	2.10	108.530
7	35.5	315	4.11	14.3761	14.3729	3.20	165.358
8	35.5	315	9.89	14.3763	14.3739	2.40	124.016
9	0.0	200	7.00	14.3761	14.3739	2.20	113.683
10	45.0	200	7.00	14.1411	14.1384	2.70	139.518
11	22.5	0	7.00	14.1401	14.1383	1.80	93.023
12	22.5	400	7.00	14.1418	14.1390	2.80	144.687
13	22.5	200	2.00	13.9872	13.9836	3.60	186.029
14	22.5	200	12.00	13.9852	13.9832	2.00	103.361
15-18	22.5	200	7.00	13.9848	13.9822	2.60	134.354

*Milligrams per square decimeter per day

independents variables (Yaro *et al.*, 2011b). A regression analysis of the objective function (corrosion rate) as function of temperature, rpm and pH leads to the following equation with 0.956 correlation coefficient:

$$CR(mdd) = 171.5 + 0.502X_1 + 0.11X_2 - 17.09X_3 + 0.76X_3^2 \quad (14)$$

Equation 14 shows that the Corrosion Rate (CR) increases with increasing temperature (X_1), rotating velocity (X_2) and with decreasing of pH (X_3). X_1 has effect about four times of X_2, but X_3 is very effective on corrosion rate especially in linear term. There is no interaction between any variable with other. The variation in coefficients is due to varying the range of each variable. Fig. 7 shows the observed values versus predicted corrosion rate values. Figure 8 and Table 3 show the relation between the potential and corrosion rate. It can be seen that the E_p is shifted to more negative direction with increasing temperature, velocity and with decreasing of pH. That means the E_p is more negative with increasing of corrosion rate. It can be seen from Table 3 that the E_p is slightly varying with variables except at very low pH region, where E_p is relatively high (in active direction) compared with other variables. Equation 15, with 0.98 correlation coefficient, shows the predicted value of E_p.

$$E_p(mV)/SCE = -859.75 - 0.247X_1 - 0.0147X_2 + 11.95X_3 - 0.529X_3^2 + 0.017X_1X_3 \quad (15)$$

Equation 15 shows that the protection potential (E_p) is slightly more negative with increasing temperature (X_1) and rotation velocity (X_2). X_2 has very low effect on E_p. pH (X_3) decreases leads to more negative of E_p. There is an interaction only between X_1 and X_3 with low effect.

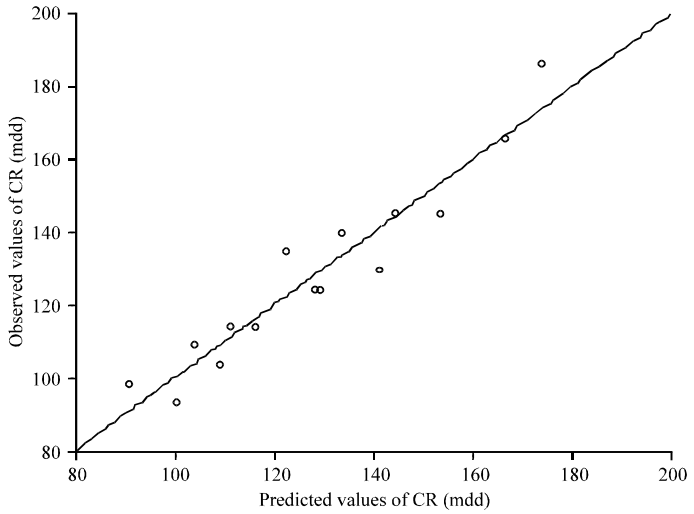

Fig. 7: Observed versus predicted values of corrosion rate (CR) of cylindrical steel specimen with different conditions

Table 3: Results of protection potentials with different conditions

Run No.	X_1	X_2	X_3	E_p, mV
1	9.5	85	4.11	-820
2	9.5	85	9.89	-800
3	9.5	315	4.11	-825
4	9.5	315	9.89	-800
5	35.5	85	4.11	-825
6	35.5	85	9.89	-800
7	35.5	315	4.11	-830
8	35.5	315	9.89	-805
9	0.0	200	7.00	-805
10	45.0	200	7.00	-810
11	22.5	0	7.00	-805
12	22.5	400	7.00	-810
13	22.5	200	2.00	-850
14	22.5	200	12.00	-790
15-18	22.5	200	7.00	-805

Polarization: The characteristic of cathodic polarization curves with variation of temperature, velocity and pH can be illustrated. Figure 8 shows polarization curves provide information about effects of changes in potential as a function of current density. Since the electrolyte is seawater (saltwater), the concentration polarization type is predominant (Jezmar, 2002). From polarization curves, it can be determined the free corrosion potential, E_{corr}, limiting current density, i_L and initial protection current density, i_{p1} (Peabody, 2001). Where E_{corr} is determined when the potential becomes approximately constant with decreasing current. The limiting current plateau is not well defined, thus the following method will be adopted to find i_L values:

$$i_L = \frac{i_1 + i_2}{2} \tag{16}$$

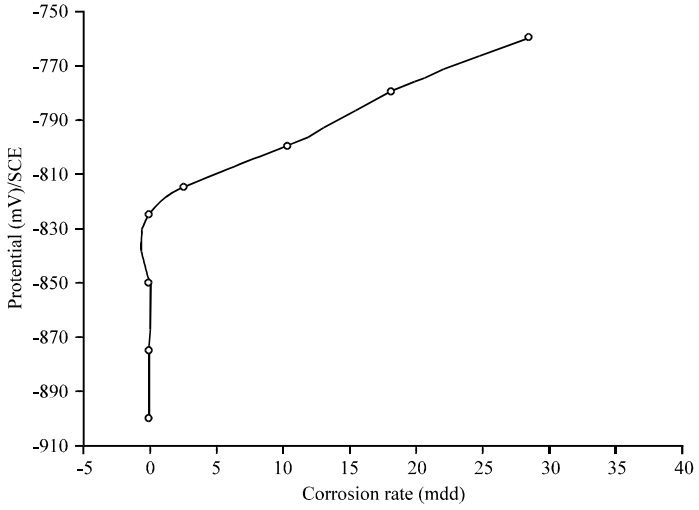

Fig. 8: Variation of protection potential (E_p) of steel in seawater with corrosion rate at X_1 = 9.5°C, X_2 = 85 rpm and X_3 = 4.11 as pH

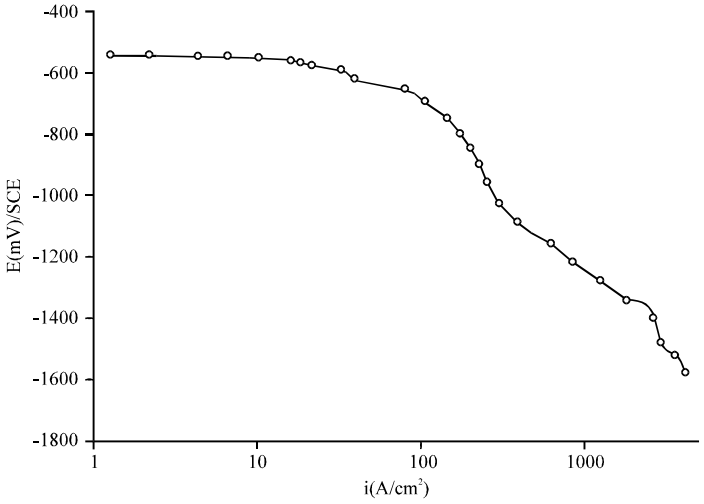

Fig. 9: Cathodic polarization curve of carbon steel in seawater at X_1 = 9.5°C, X_2 = 85 rpm and X_3 = 4.11

where, i_1 and i_2 are the current associated with E_1 and E_2. i_{p1} can be determined by intersect of E_p (which is determined previously) with cathodic polarization curve (Trethewey and Chamberlain, 1996). From Fig. 9 and other polarization curves one can see that the E_{corr} is more negative with increasing temperature and with decreasing velocity and pH. While i_L increases with increasing temperature and velocity and with decreasing pH. The high value of i_L means the high corrosion and vice versa. i_{p1} is also proportional to the corrosion rate where in high corrosive media (high temperature and velocity and low pH), one can see that the i_{p1} is largely raised in contrast to the E_p which is slightly varying with conditions as mentioned previously. The results of E_{corr}, i_L and i_{p1} are summarized in Table 4 for various conditions.

Table 4: Results of E_{corr}, i_L and i_{p1} which obtained from polarization curves.

Run No.	X_1	X_2	X_3	E_{corr}, mV	i_L, μA/cm^2	i_{p1}, μA/cm^2
1	9.5	85	4.11	-546	206.3	180.3
2	9.5	85	9.89	-510	140.4	117.5
3	9.5	315	4.11	-529	308.6	253.5
4	9.5	315	9.89	-496	156.7	177.8
5	35.5	85	4.11	-569	234.1	230.0
6	35.5	85	9.89	-545	147.7	134.3
7	35.5	315	4.11	-554	302.0	275.4
8	35.5	315	9.89	-518	184.0	190.5
9	0.0	200	7.00	-514	188.4	186.2
10	45.0	200	7.00	-591	229.0	231.7
11	22.5	0	7.00	-610	118.9	81.0
12	22.5	400	7.00	-520	251.2	236.6
13	22.5	200	2.00	-590	346.7	337.3
14	22.5	200	12.00	-500	139.6	121.8
15-18	22.5	200	7.00	-545	237.1	210.8

Table 5: Initial and steady values of protection current

Run No.	X_1	X_2	X_3	i_{P1} initial value (μA/cm^2)	i_P steady value (μA/cm^2)	Stability time (min)
1	9.5	85	4.11	180.3	156.2	127
2	9.5	85	9.89	117.5	97.4	152
3	9.5	315	4.11	253.5	212.1	131
4	9.5	315	9.89	177.8	153.0	150
5	35.5	85	4.11	230.0	186.2	115
6	35.5	85	9.89	134.3	112.4	130
7	35.5	315	4.11	275.4	224.1	118
8	35.5	315	9.89	190.5	164.3	126
9	0.0	200	7.00	186.2	161.0	146
10	45.0	200	7.00	231.7	187.7	128
11	22.5	0	7.00	81.0	61.3	139
12	22.5	400	7.00	236.6	191.6	146
13	22.5	200	2.00	337.3	258.6	168
14	22.5	200	12.00	121.8	102.4	109
15-18	22.5	200	7.00	210.8	176.5	138
19*	22.5	150	7.00	192.7	166.8	121

* Run 19 is added to check effect of velocity on stability time

Protection current i_P: The results obtained from polarization curves for current required for cathodic protection were listed in Table 4. These values were almost unstable with time due to scale formation on the surface of steel that reduces the current consumption. The data shows decrease the cathodic protection current density from an initial value (i_{P1}) to a fairly steady values i_P. For high temperature regions, i_P is more stable than for low temperature regions. This is because the high temperatures enable to form the scales on the surface greater than the low temperatures. With increasing velocity relatively (0-150 rpm), i_P is more stable due to increase the corrosion products with increasing velocity. Further increasing in velocity leads to remove the scales and delay in stability of i_P. i_P is more stable with reducing the pH from 7 to 4.11 due to increasing the corrosion product with lowering of pH. But with very low value of pH i_P becomes less stable due to the dissolution of scale. The results obtained from figures, such as Fig. 10; of protection currents for various conditions are summarized in Table 5.

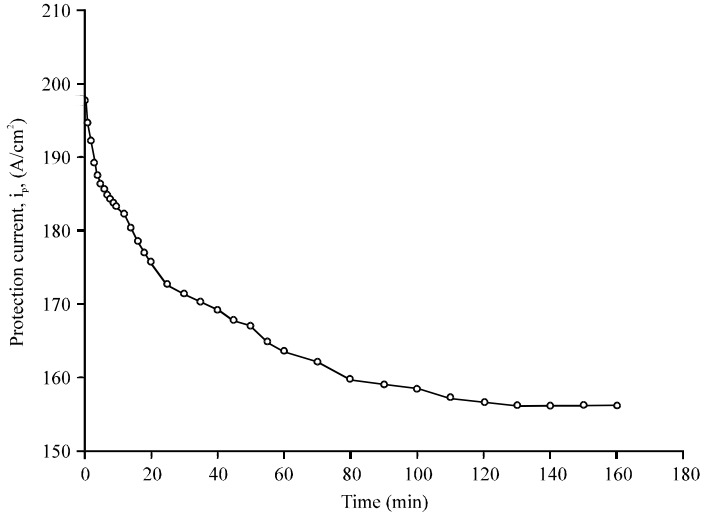

Fig. 10: Variation of protection current density versus time of carbon steel in seawater at X_1 = 9.5°C, X_2 = 85 rpm and X_3 = 4.11

CONCLUSION

The study of sacrificial anode cathodic protection of short steel tube using zinc strip extended axially in the pipe revealed that under the present range of conditions, the rate of zinc consumption increases with increasing time, temperature and flow rate and with decreasing of pH. The zinc consumption with very low pH is very high and the cathodic protection becomes unreliable. The study of impressed current cathodic protection of rotating vertical steel cylinder in sea water showed that the protection potential and protection current are highly depend on variable of research.

ACKNOWLEDGMENT

This study, was supported by Baghdad University, Chemical Engineering Department which is gratefully acknowledged.

REFERENCES

Ahmed, M.J., A.A. Khadom and A.H. Kadhum, 2009. Optimization hydrogenation process of D-glucose to D-sorbitol over raney nickel catalyst. Eur. J. Sci. Res., 30: 294-304.

Alagbe, M., L.E. Umoru, A.A. Afonja and O.E. Olorunniwo, 2006. Effects of different amino-acid derivatives on the inhibition of NST-44 mild steel corrosion in lime fluid. J. Applied Sci., 6: 1142-1147.

Bazargan-Lari, R. and Y. Bazargan-Lari, 2009. Investigation of failure and corrosion in pipelines and tanks used in ice-cream factory: The case study. Trends Applied Sci. Res., 4: 56-61.

Ekuma, C.E. and N.E. Idenyi, 2007. Statistical analysis of the influence of environment on prediction of corrosion from its parameters. Res. J. Phys., 1: 27-34.

Ekuma, C.E., 2008. Statistical model for the evaluation of corrosion behaviour of Al-Sn binary alloy systems. Trends Applied Sci. Res., 3: 25-35.

Ekuma, C.E., N.E. Idenyi and S.I. Neife, 2007. Comparative analysis of the corrosion susceptibility of cast Al-Mn alloys in acidic environments. Res. J. Environ. Sci., 1: 185-190.

Ekuma, C.E., N.E. Idenyi, F.K. Onwu and A.E. Umahi, 2008. The influence of media concentrations on the passivation layer characteristics of Al-Zn alloys in brine environment. Asian J. Sci. Res., 1: 113-121.

Jezmar, J., 2002. Monitoring methods of cathodic protection of pipe lines. J. Corros. Meas., 2: 13-16.

Khadom, A.A., 2010. Reaction kinetics of zinc as a sacrificial anode for cathodic protection of copper pipes carrying saline water in presence of bacteria. World Applied Sci. J., 10: 364-369.

Khadom, A.A., A.S. Yaro and A.H. Kadhum, 2010. Corrosion inhibition by naphthylamine and phenylenediamine for the corrosion of copper-nickel alloy in hydrochloric acid. J. Taiwan Inst. Chem. Eng., 41: 122-125.

Khadom, A.A., A.S. Yaro, A.A.H. Kadum and A.S. Altaie, 2009. Mathematical modeling of corrosion inhibition behavior of low carbon steel in HCl acid. J. Applied Sci., 9: 2457-2462.

Konsowa, A.H. and A.A. El-Shazly, 2002. Rate of zinc consumption during sacrificial cathodic protection of pipelines carrying saline water. Desalination, 153: 223-226.

Lindley, C. and W.J. Rudd, 2001. Infuence of the level of cathodic protection on the corrosion fatigue properties of high-strength welded joints. Mar. Struct., 14: 397-402.

Okeniyi, J.O., O.A. Omotosho, O.O. Ajayi, O.O. James and C.A. Loto, 2012. Modelling the performance of sodium nitrite and aniline as inhibitors in the corrosion of steel-reinforced concrete. Asian J. Applied Sci., (In Press).

Omotosho, O.A., O.O. Ajayi, O. Fayomi and V.O. Ifepe, 2012. Evaluating the deterioration behaviour of mild steel in 2 M sulphuric acid in the presence of *Butyrospermum parkii*. Asian J. Applied Sci., 5: 74-84.

Parthiban, G.T. Parthiban, T. Ravi, R.V. Saraswathy, Palaniswamy and N.V. Sivan, 2008. Cathodic protection of steel in concrete using magnesium alloy anode. Corros. Sci., 50: 3329-3335.

Peabody, A.W., 2001. Peabody's control of pipeline corrosion. 2nd Edn., NACE press, USA.

Shrier, L.L., 2000. Corrosion. Vol. 2, Newnes-Butterworth, UK.

Trethewey, K.R. and J. Chamberlain, 1996. Corrosion for scientist and engineering. 2nd Edn., Addison Wisely publishing, USA Pages: 446.

Yaro, A.S. H. Al-Jandeel and A.A. Khadom, 2011a. Cathodic protection system of copper-zinc-saline water in presence of bacteria. Desalination, 270: 193-198.

Yaro, A.S., A.A. Khadom and H.F. Ibraheem, 2011b. Peach juice as an anti-corrosion inhibitor of mild steel. Anti-Corros. Methods Mater., 58: 116-124.

Zahran, R.R. and G.H. Sedahmed, 1997. Galvanic corrosion of zinc in turbulently moving saline water containing drag reducing polymers. Mater. Lett., 31: 29-33.